Starch-based superabsorbent hydrogel: Synthesis, characterization and properties evaluation in agricultural field

Highlights

The synthesis, characterization, and property evaluation of starch-based hydrogel are highlighted in this chapter to overcome the drawbacks of conventional petroleum resource-based hydrogels. The first part of the chapter deals with the optimization of the synthetic procedure to obtain a highly swell able material with a low amount of synthetic monomer. Subsequently, this chapter includes the characterization of the synthesized material by using various analytical and spectroscopic techniques. Further this chapter deals with the effect of the hydrogel on various soil properties for agricultural applications. In addition, biodegradation study of the synthesized hydrogel was also evaluated to overcome the drawbacks of conventional non-degradable polymeric materials. Lastly, the chapter reports the evaluation of the encapsulation efficiency of urea in urea-loaded hydrogel and its control release ability to address the pollution and the economic loss caused by most of the water-soluble fertilizers.

Parts of this chapter are published as

[1] Sarmah, D. and Karak, N. Biodegradable superabsorbent hydrogel for water holding in soil and controlled-release fertilizer. *Journal of Applied Polymer Science,* 137(13): 48495, 2020.

2.1. Introduction

Chapter 1 demonstrated hydrogel as a promising material due to its vast applications including controlled release of fertilizer in agriculture [1], personal hygiene materials such as baby diapers and female napkins [2], controlled drug delivery system [3], tissue engineering [4], wastewater treatment [5,6], biosensors [7], soft lenses [8], water holding in soil [9], etc. Due to these wide spectrums of applicability, the productions of hydrogels have received immense attention among both industrialists and researchers over the last few decades. However, synthetic monomer-based hydrogels become a threat to the society and urgent replacement of these materials with renewable resource-based materials is the need of the hour. In this context, polysaccharide-based hydrogels have received huge importance due to their hydrophilicity, biocompatibility, and biodegradability [10,11]. Literature advocates the preparation of large numbers of polysaccharide-based hydrogels with high swelling ability [12,13]. Although, constant efforts have been made to obtain bio-based hydrogel but insufficient amount of bio-based components restricts its applications purpose in various fields [14,15]. Thus, to address the issues related to the growing environmental degradation as discussed, it is necessary to reduce the amount of synthetic monomers as much as possible along with higher swelling ability. Thus, a high swell able starch-based hydrogel was synthesized by using a solution polymerization technique in the presence of acrylic acid (AA) as water-soluble monomer with *N, N*-methylene bisacrylamide (MBA) as a cross-linker, and as an initiator. All the amount of the reactants was optimized to obtain the hydrogel with high swelling ability to make it suitable for agricultural applications. The performance characteristics of the material such as swelling ability in distilled water, and saline solution were evaluated to justify the efficiency of the material.

The agricultural sector of the world depends on rainfall and the uncertainties in the frequency of rainfall in arid and semiarid areas result in scarcities of water, which lead to uncontrollable crop loss time to time [16]. Owing to extraordinary water absorbing capacity, the synthesized hydrogel was employed to study the water-holding capacity of the soil. After the incorporation of hydrogel, it can affect other soil properties such as porosity, soil density, etc. The addition of only a small amount of the hydrogel enhanced these properties significantly.

Along with water, fertilizer is also an important factor that greatly affects the production of agriculture [1]. Nitrogen is one of the most essential macronutrients for the production

of various crops and urea is the most widely used nitrogen-containing fertilizer [17]. But only a very small percentage of applied urea is used by the plants due to its high-water solubility. This fact senses the use of a very high amount of urea, which not only increases the cost but also pollutes the surface as well as the ground water. Thus, slow-release-impregnated urea can increase the efficiency of nitrogen uptake of plants and can reduce serious environmental problems. Along with the large water retention ability the synthesized hydrogel exhibits extraordinary encapsulation efficiency for urea and can slow the release of this entrapped material with time. In addition to this, the hydrogel exhibits noteworthy biodegradability and this property make it suitable for agricultural applications.

Thus, the hydrogel acquires all the potential properties to quantify it as a suitable material for agricultural applications with high water-holding capacity and nutrient-carrier ability.

2.2. Experimental

2.2.1. Materials

Tapioca starch was supplied by Hindustan Gum & Chemicals Ltd, Bhiwani, India. It is a polysaccharide extracted from cassava roots. It is white powder with insoluble in water at room temperature. However, it is dispersible in water at high temperature and was used to prepare the main hydrogel network.

AA with molecular weight 72.06 g/mol and 1.05 g/cm^3 density was procured from SRL, India, and was used without further modification.

APS is a white solid with molecular weight 228.18 g/mol. It was purchased from SRL, India and its aqueous solution was used to initiate the reaction.

MBA with molecular weight 154.17 g/mol was from SRL, India, and used as the cross-linking agent without any modification.

Sodium hydroxide (NaOH) pellet with 97% purity was brought from Merck, India. The aqueous solution of NaOH was used for the neutralization purpose of the prepared hydrogel.

Methanol (CH_3OH) was acquired from Merck, India. It was used to wash the synthesized hydrogel before drying.

Sodium chloride (NaCl) was brought from Merck, India and it was utilized to investigate the effect of salt on swelling.

Calcium chloride ($CaCl_2$) was purchased from Merck, India and its salt solution was used to study the effect of salt on swelling of the hydrogel.

Urea is nitrogen containing fertilizer and purchased from Merck. It was used to study the controlled release ability of hydrogels.

4-Dimethylaminobenzaldehyde (DMAB) was purchased from Merck, India. Its molecular weight is 149.19 g/mol and is used for the determination of the concentration of urea.

Hydrochloric acid (HCl) was obtained from Merck, India. It was used in the determination of the concentration of released urea.

The soil used in this chapter was collected from Tezpur University campus, India. The soil was dried under sunlight for 72 h, and the unwanted dirt particles were removed manually. It was silty and sandy (pH 6.5) with a carbon content of 2.45%, a nitrogen content of 0.23%, a hydrogen con tent of 0.21%, and a total organic matter content of 4.22% [18]. Before analysis, the soil was turned into powdered form.

2.2.2. Methods

2.2.2.1. Synthesis of the superabsorbent hydrogel (SAH)

The bio-based SAH was synthesized by free radical polymerization reaction between the various reactants namely starch and AA in the presence of APS initiator and MBA cross-linker. To proceed the reaction tapioca starch was added with 10 mL of 0.067N NaOH solution in a three-neck round bottom flask. To provide an inert atmosphere N_2 gas was purged continuously into the reaction chamber. The reaction temperature was increased gradually up to 45 °C and at that temperature 1 mL AA in 1 mL and 0.01 g of MBA was added under continuous stirring. Then the temperature was increased to 70 °C and was maintained until the starch became transparent. Thereafter, the reaction temperature was reduced to 55 °C and 0.04 g of APS with 1 mL of water was added to initiate the polymerization reaction. Subsequently, the temperature was again raised to 70 °C. The gel formation was started after 30 min and completed within the next 2 min. Then, immediately 1.7 mL of 8 N NaOH was mixed with the gel under vigorous stirring for 15 min. The prepared gel was allowed to swell in an excess amount of water for 24 h. Then it was washed with CH_3OH to remove the unreacted components. Finally, the hydrogel was oven-dried at 90 °C and transform to powder form for further study. Three compositions of the hydrogels were prepared and encoded as SAH 1, SAH 2, and SAH 3

as tabulated in **Table 2.1**. Only AA based hydrogel (without the inclusion of starch) was prepared for comparison purpose and encoded as PAA hydrogel.

Table 2.1. Variation of different reactants used in synthesis of SAH.

Sample code	Starch content (g)	AA content (g)	MBA content (g)	APS content (g)	Solid content (%)
SAH 1	1	0.78	0.01	0.04	14.70
SAH 2	1	1.05	0.01	0.04	17.16
SAH 3	1	2.10	0.01	0.04	25.91
PAA hydrogel	----	1.05	0.01	0.04	8.83

2.2.2.2. Preparation of urea-encapsulated hydrogel

The urea-encapsulated hydrogel was prepared by grafting starch with AA in the presence of urea by a similar procedure as stated above. Briefly, an amount of 1 g starch was mixed with 10 mL of 0.067 N NaOH and 4 g of urea in the same arrangement as above reaction chamber under the N_2 atmosphere. After the starch-urea mixture become transparent as described above, all the reactants were added subsequently. Then, 1.05 g of AA in 1 mL water with 0.01 g of MBA was mixed with the above mixture at 45 °C with a constant stirring. When the starch-urea mixer became transparent AA with MBA was added as described above, along with subsequent addition of the initiator to initiate the reaction and stirred at 70 °C to form a solid gel-like product. The gel was allowed to swell with 50 mL of water overnight. Then it was dried in an oven at 70 °C and the urea release profile was studied in distilled water.

2.2.3. Structural analysis

The Fourier transformed infrared (FTIR) spectra of SAHs were recorded with the help of a Nicolet (Madison, USA) impact 410 spectrophotometer using KBr pellets over the range of 4000-400 cm^{-1}. XPS study of SAH 2 was recorded on ESCALAB 220 XL spectrometer using 100 eV and 40 eV constant analyzer energies for survey spectra and high-resolution spectra, respectively.

2.2.4. Thermal study

The thermogravimetric analysis (TGA) of starch and the synthesize hydrogel were done using a TGA-4000 (PerkinElmer) in a temperature range of 32-720 °C under the nitrogen atmosphere with a flow rate of 30 mL min^{-1} and at a heating rate of 10 ℃ min^{-1}.

2.2.5. Swelling test

To determine the swelling capacity, 50 mg of dry hydrogel was immersed in excess amount of the desired liquid medium. The swollen hydrogel was withdrawn from the liquid medium after equilibrium swelling. The loosely associated excess liquid was wiped out using a blotting paper and the increased weight of the swollen gel was measured. Then, the swelling capacity was determined by using the following equation.

$$\textbf{Swelling} = (W_s - W_d)/W_d \quad \text{---------- Eq. 2.1}$$

where W_s and W_d are the weight of the hydrogel after and before swelling, respectively.

The swelling characteristics of the synthesized hydrogel were also studied in salt solutions of NaCl (different concentrations) and $CaCl_2$.

2.2.5.1. Study of effect of cross-linker, initiator on swelling

To examine the effect of cross-linker on swelling, the amount of cross-linker was varied from 0.01 g to 0.03 g keeping constant amount of starch, AA, APS, and NaOH solution. Similarly, to study the effect of the initiator, its amount was varied from 0.04 g to 0.08 g, without changing other parameters.

2.2.6. Biodegradation of the synthesized hydrogel

The biodegradation study of the synthesized hydrogels was performed using the soil burial method. For this experiment, a calculated amount hydrogel was taken inside a few paper cups containing 60 g of powdered soil. Thereafter, 50 mL of water was added to each cup and buried inside the soil at a depth of 7-9 cm. After a particular time-interval, the hydrogel samples were taken out, washed gently to remove the attached soil, dried, and weighed. The weight loss percentage at each time was determined by using the following relationship.

$$\textbf{Weight loss (\%)} = (W_i - W_t)/W_i \times 100 \quad \text{---------- Eq. 2.2}$$

where W_i and W_t are the initial weight and the weight after degradation, respectively.

2.2.7. Water-absorption capacity of soil

To determine the water-holding capacity of the soil, a fixed quantity (10 g) of powder, air-dried soil was treated with 0.05 g of each of the three compositions of the hydrogels (SAH 1, SAH 2, and SAH 3), separately. One sample of soil without hydrogel was kept for comparison purposes. Four plastic beakers having small holes at the bottom were taken and both treated and untreated soils with 30 mL of water were placed in them. The weights of these soil samples were taken after 24 h and the water-holding capacity was measured using the following equation.

$$\textbf{Water-holding capacity (\%)} = (W_t - W_i)/W_i \times 100 \text{ ----------Eq. 2.3}$$

where W_t is the weight of the soil after 24 h and W_i is the weight of the before the addition of water.

2.2.8. Determination of density and porosity of the treated soil

For the determination of the soil density of the representative soil, 20 g of dried powered soil was taken. The particle density of this soil was measured using a pycnometer as per the standard method before any treatment. Subsequently, for the determination of the bulk density, 20 g of dry-powered soil with the three compositions of the hydrogels were taken separately in three beakers with holes at the bottom. Soil without any hydrogel was kept in the same way for comparison purposes. 30 mL of water was mixed with each of the beakers and kept in the open air under sunlight for 20 days to facilitate drying. Weight of the selected amount of the air-dried control soil was taken and volume was measured. The bulk density of the soil was determined by using the following formula.

$$\textbf{Bulk density = Weight of soil/Volume of the soil ---------- Eq. 2.4}$$

Based on the particle density and the bulk density values, the percentage of porosity of the soil was determined using the following formula [9].

$$\textbf{Porosity (\%) = [1 – (bulk density/particle density)] × 100---------- Eq. 2.5}$$

2.2.9. Study of urea-released profile

For the estimation of urea concentration in water, DMAB was used as a colorimetric

reagent. This compound can form a greenish yellow color complex under acidic conditions, in accordance with **Ehrlich** reaction and shows λ_{max} at 430 nm [19]. A standard curve was prepared by plotting concentration versus absorbance, by detecting a known concentration of urea solutions. To detect the concentrations of urea in an aqueous solution, 1 mL of urea-containing solution was taken in a glass vial with 1.8 mL of 20 g/L DMAB in CH_3OH solution. Concentrated HCl (0.067 mL) was added to the above mixture and shaken manually for 5 min to ensure the completion of the reaction. Thereafter the absorbance of the mixture was determined at λ_{max} of 430 nm using a UV–vis spectrophotometer.

Before the study, the urea release, the oven-dried urea-loaded hydrogel was wash with 20 mL of distilled water to remove the surface-adhered urea. The washed-out urea was detected from the standard curve and the encapsulation efficiency was calculated by using the following relationship.

$$\textbf{Encapsulation Efficiency (\%)} = (1 - W_1/CW_0) \times 100 \text{ ---------- Eq. 2.6}$$

where W_1 is the washed-out urea content, W_0 is the dry weight of hydrogel, and C is the weight of urea initially loaded during the polymerization reaction.

To study the urea release profile in water urea-encapsulated hydrogel was dipped in 1000 mL of tap water in a glass beaker. An amount of 1 mL urea solution was taken from above at different intervals (5, 10, 15, 20, 25, and 30 days) for estimating the concentration of the released urea in water. Then, the concentration of the released urea was determined by comparing it with the standard curve as done in the case of encapsulation efficiency of urea.

2.3. Results and discussion

2.3.1. Synthesis of the SAH

The starch-AA based hydrogel was synthesized by free radical polymerization reaction using water as solvent. In this solution polymerization technique, poly(acrylic acid) (PAA) chains were grafted on the starch backbone using APS as the initiator and MBA as a cross-linking agent, as shown in **Scheme 2.1**. In an inert atmosphere, the initiator APS decomposed into primary radicals (sulfate radicals). Afterward, these radicals displaced the H radicals from the primary hydroxyl of starch to form alkoxy radicals. Subsequently, the initiator also reacted with the AA monomers to form new radicals

which can also react with other monomers to contribute to the chain growth. Thus, the AA monomers converted to PAA chains and grafted on the alkoxy radicals of the starch backbone. Meanwhile, the vinyl groups of the cross-linker MBA reacted with the PAA chains to form a cross-linked network structure. Finally, polymeric chains terminated on depletion of all the monomers [20].

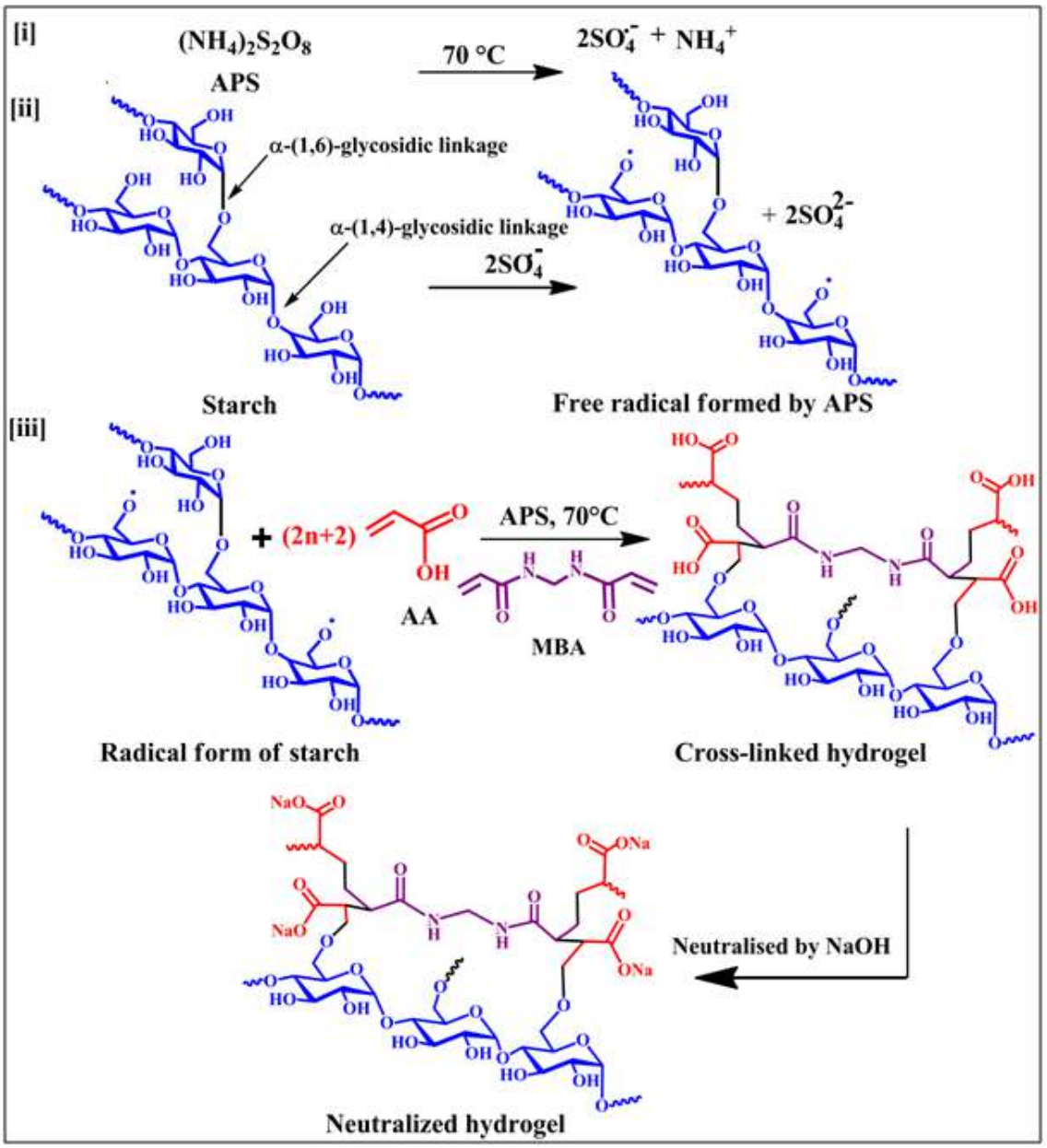

Scheme 2.1. Synthetic route of SAH.

2.3.2. Structural analysis

The structural analysis of the hydrogels was carried out by using FTIR and XPS.

2.3.2.1. FTIR study

The FTIR spectra of starch and PAA and the three compositions of the hydrogels are shown in **Figure 2.1.(a** and **b).** From the spectra, the interactions between starch with other reactants such as AA and MBA could be easily understood. The appearance of several characteristic bands in the FTIR spectrum of the hydrogel proved that AA is successfully grafted on the starch moieties. For instance, the band at 3433 cm^{-1} designated the O─H stretching frequency, while the absorptions at 2927 cm^{-1} and 2850 cm^{-1} represented C─H asymmetric and symmetric stretching frequencies. These two are the important bands for both starch and AA moieties in the hydrogel. Further, the band at 1715 cm^{-1} was attributed to the carbonyl group of AA moiety. Furthermore, the FTIR spectrum of hydrogel showed a band at 1563 cm^{-1}, which was absent in bare starch [12]. This is due to the presence of the N─H group of the cross-linker, MBA. The band at 1130 cm^{-1} is due to the C─O─C linkage of the starch moiety, while the band at 1327 cm^{-1} is due to the stretching vibration of ─H_2C─O─CH_2─, and ether linkages produced in between the primary hydroxyl group of starch and the poly(acrylic acid) moieties [21,22].

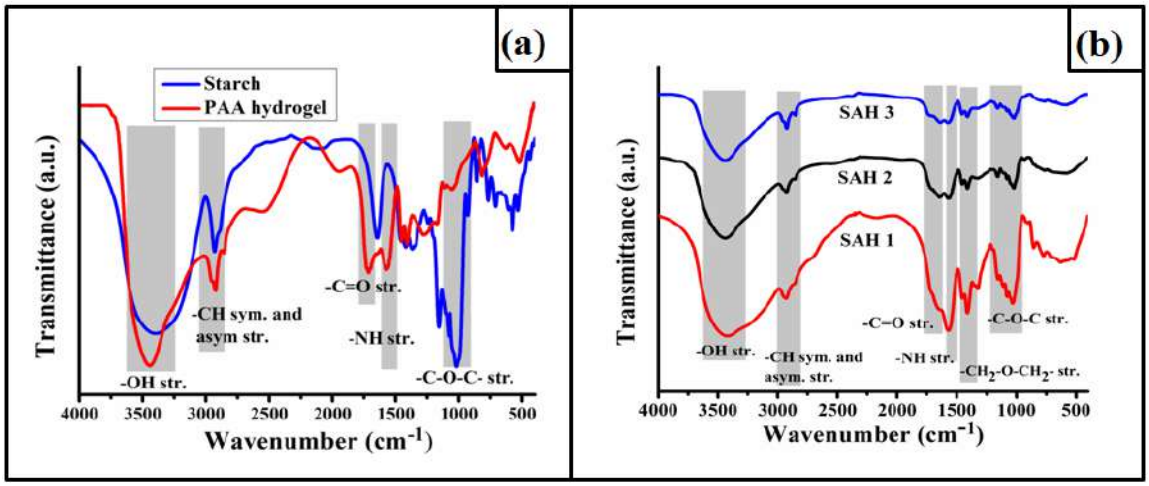

Figure 2.1. FTIR spectra of (a) starch and PAA, and (b) SAH 1, SAH 2, and SAH 3.

2.3.2.2. XPS study

XPS study was carried out to study the structure of SAH 2 hydrogel (**Figure 2.2.a**). The hydrogel contains C, N, O, and Na and their atomic fractions are 51.68%, 0.25%, 42.46%, and 5.61%, respectively. However, the high-resolution XPS spectra provide evidence for the presence of different charged and uncharged groups as shown in **Figure 2.2.b-d.** After deconvolution, the C 1s peak is converted into four peaks at 284.68eV (C–H and C–C), at 284.63 eV, 285.58 eV (C–N and C–O–C), 286.18 eV (O–C–O, C–O,

and C=O) and at 288.00 eV (COO^-) **Figure 2.2.b**. Thus, the presence of starch and AA in the structure is clearly evident from these peaks. The O 1s also provides similar information as after deconvolution three peaks are obtained as shown in **Figure 2.2.c**. The deconvoluted O 1s peaks can be attributed to the (C–O, C–O–C), (C–O–C and C=O), COO^- groups at binding energies 531.11 eV, 532.61 eV, and 533.27 eV, respectively (**Figure 2.2.d)** [20]. Thus, the high-resolution XPS spectra provide evidence for the formation of ether linkages between starch and AA in addition to the presence of these groups. Moreover, after deconvolution, the N 1s provides peaks confirming the presence of MBA in the structure. The presence of Na 1s is due to the entrapped Na^+ from NaOH solution used in neutralize the COO^- groups of AA (**Figure 2.2.e)**.

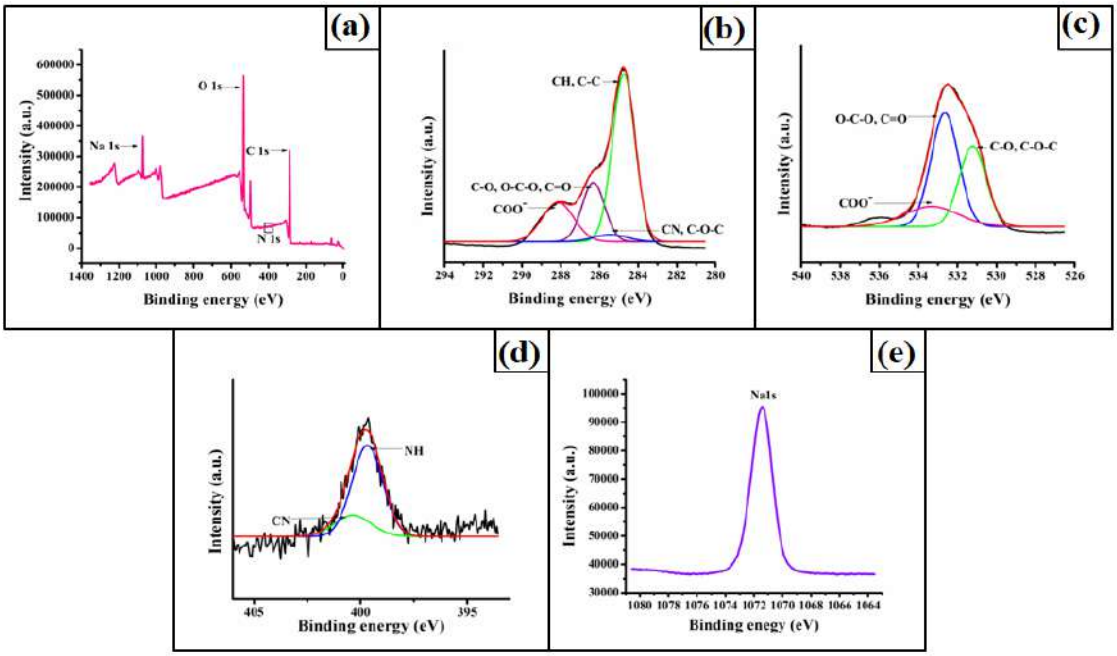

Figure 2.2. XPS spectra of (a) SAH 2; (b) C 1s, (c) O 1s, (d) N 1s, and (e) Na 1s, for SAH 2.

2.3.3. Thermal degradation study

The thermograms as well as their first derivatives (DTG) of pristine starch and SAH 2 are shown in **Figure 2.3.a** and **b.** The initial degradation temperature for both pristine starch and SAH 2 is due to the moisture present in the hydrogel (SAH 2) [23]. Pristine starch showed a degradation temperature at around 320 °C, which can be attributed to the degradation of its backbone. In the case of SAH 2, the degradation temperature at around 280 °C-320 °C is associated with the decomposition of various chemical bonds such as hydroxyl, ester, and ─C─O─C─ groups of SAH 2. Again, the last step is the degradation

of the remaining component, PAA chains with maxima at around 450 °C. SAH 2 was more resistant toward thermal decomposition than the pristine starch.

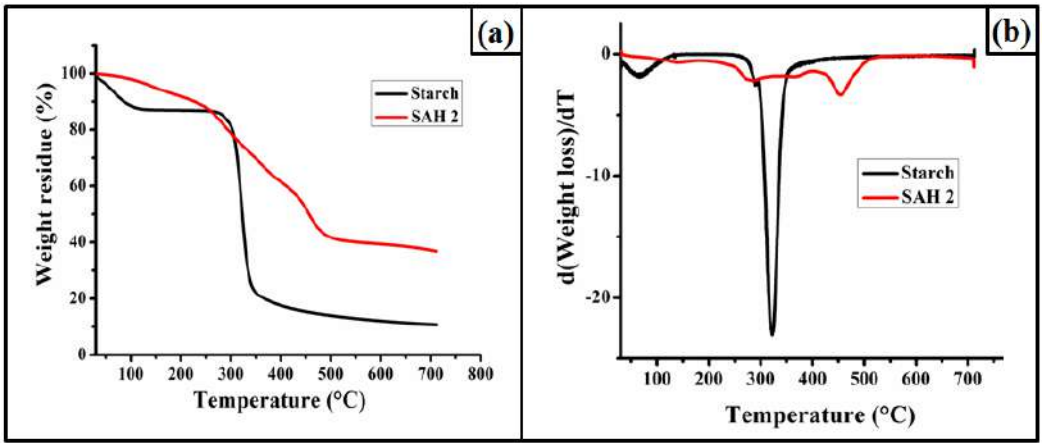

Figure 2.3. (a) TGA thermograms, and (b) DTG curves of starch and SAH 2.

2.3.4. Swelling study

The swelling ability of the three compositions of the hydrogels is shown in **Figure 2.4.**

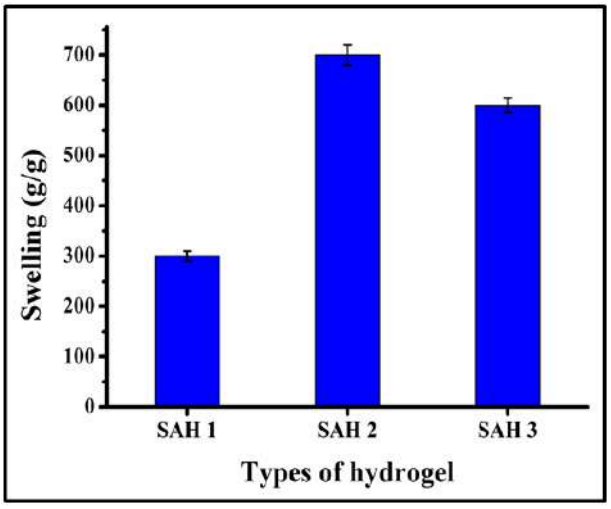

Figure 2.4. Swelling of SAH

Among the three compositions, the highest absorbing capacity was observed when the starch-to-AA weight ratio was 1:1.05. After decreasing the AA content from 1.05 g to 0.78 g, a significant decrease in the swelling ability was observed. This may be due to the insufficient amount of AA in the matrix to form optimum hydrogel. This may also be because of the lowering concentration of the total solid in the reaction mixture (**Table 2.1**). Hence, the amount of initiator is more, and as a result, the molecular chain length is reduced resulting in a lower swelling value. However, with the increase in the AA

content, the swelling capacity has increased due to the presence of more numbers of hydrophilic COO^- groups on the AA chains. But when the amount of AA was high (2.10 g), the solid content in the reaction mixture was also high (25.91%). As the concentration of the monomers increased inside the reactor, the polymerization increased to a very high extent, and hence chain coiling and cross-linking increased resulting in a very hard hydrogel. As the gel strength increased, the pores between the cross-linked points are expanded to a limited extent. As a result, space decreased for water molecules [24]. The visual appearance of the increased cross-linking density of these hydrogels with the increasing concentration of AA content is shown in **Figure 2.5**.

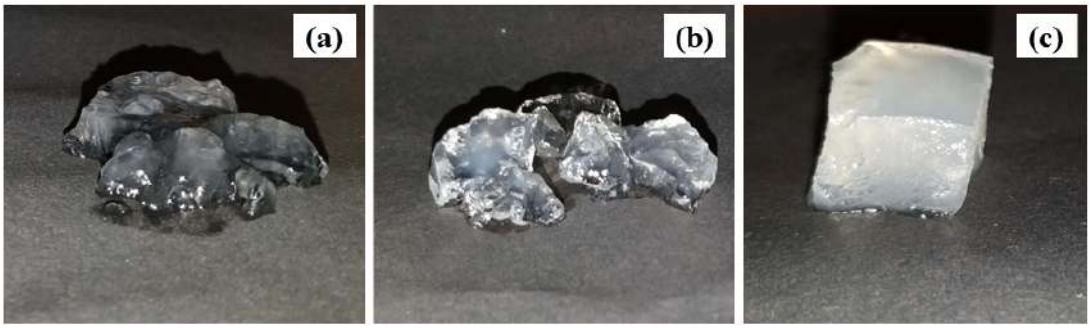

Figure 2.5. Digital photographs of hydrogels showing dimensional stability and strength of (a) SAH 1, (b) SAH 2, and (c) SAH 3.

2.3.4.1. Effect of cross-linker on swelling

The cross-linker plays a very significant role in regulation of various properties of hydrogels. Cross-linker forms a three–dimensional (3D) network structure by connecting the individual polymer chains to form pores inside the polymer matrix. The concentration of the cross-linker can affects strength of the gel network, thereby influence the swelling capacity. The effect of cross-linkers on the absorbing capacity of the SAH is depicted in **Table 2.2**. The swelling ability of hydrogel was found to be the highest at a cross-linker amount 0.01 g. The swelling ability was lowered upon further increase in cross-linker amount from 0.01 g to 0.03 g. The cross-linking density increases with the increase in cross-linker concentration, and this, in turn, decreased the swelling ability of the hydrogel. As with an increase in the cross-linking density, the distance between the cross-linked point decreases and this makes the hydrogel hard and compact. As a result, the pore between the cross-linked points cannot be expanded to a high extent, and hence area in pores decreases for the adsorption of water, thereby decreasing the swelling ability of the hydrogel [25]. However, below 0.01g cross-linker

was unable to connect the required individual sites of the polymer to form a stable gel.

Table 2.2. Influence of cross-linker on swelling of hydrogel

Starch content (g)	AA content (g)	MBA content (g)	APS content (g)	Swelling (g/g)
1	1.05	0.01	0.04	700±20
1	1.05	0.02	0.04	322±10
1	1.05	0.03	0.04	284±05

2.3.4.2. Effect of initiator on swelling

The initiator produces free radicals by thermal decomposition, thereby initiating the polymerization of monomer molecules. The concentration of initiator significantly influences the swelling of the hydrogel. The swelling of SAH is the maximum at an APS amount of 0.04 with respect to the other reactants, and this is considered the optimum concentration of the initiator (**Table 2.3).**

Table 2.3. Influence of initiator on swelling of the hydrogel

Starch content (g)	AA content (g)	MBA content (g)	APS content (g)	Swelling (g/g)
1	1.05	0.01	0.04	700±20
1	1.05	0.01	0.06	542±15
1	1.05	0.01	0.08	468±10

This is also the least amount of concentration of the initiator and below which the effective polymerization reaction was not possible. This may be due to the formation of insufficient amount of free radicals that are required for the generation of active monomer radicals for the polymerization process. Again, at more than this concentration of the initiator, the swelling ability of the hydrogel was reduced. This may be due to the generation of large numbers of free radicals that create many active monomer radicals, and the results of many small polymer chains are formed as the concentration of the monomer was constant. This decreased swelling capacity of the hydrogel is due to less numbers of pores with coiled chains of the matrix [25].

2.3.4.3. Swelling mechanism of the hydrogel

The molecular representation of swelling mechanism with the visual appearance of the hydrogel before and after swelling is shown in **Scheme 2.2.**

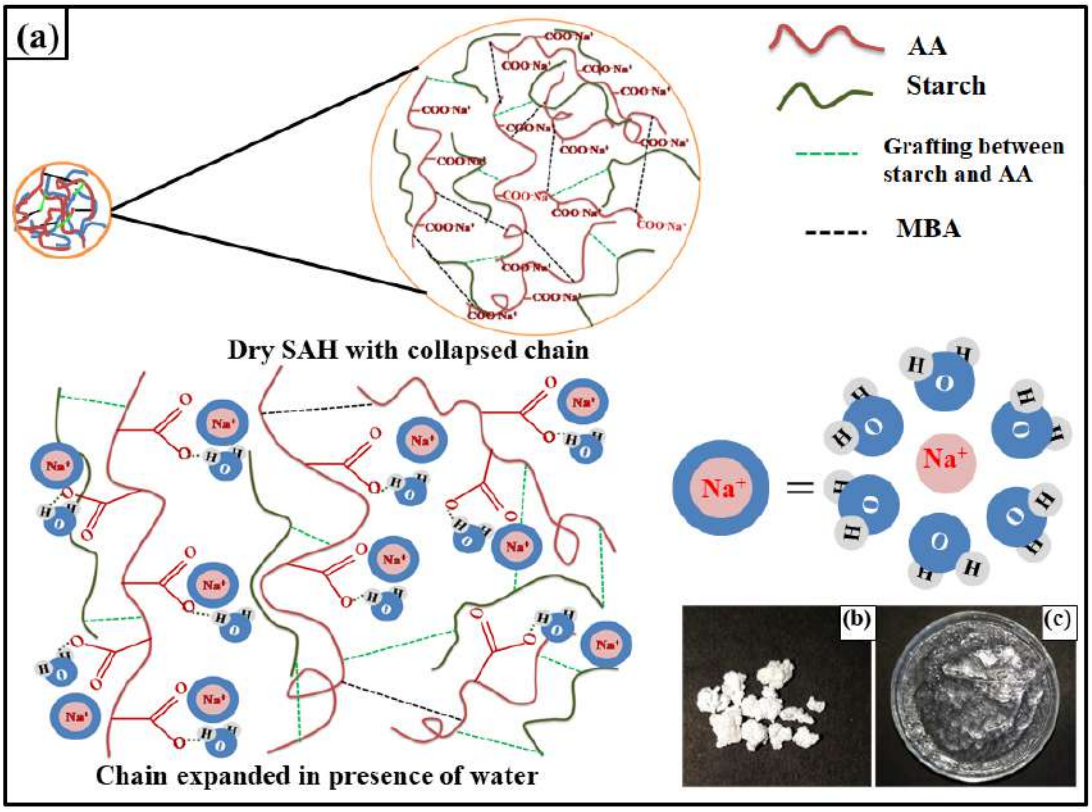

Scheme 2.2. (a) The molecular representation of swelling mechanism with the visual appearance of the hydrogel before and after swelling, and images of (b) dry hydrogel and (c) swollen hydrogel.

On neutralization of the hydrogel with aqueous NaOH solution, the H^+ ions of the carboxylic groups of AA moiety were replaced by Na^+ ions, thus maintaining the overall electrical neutrality within the polymeric chains. Upon contact of hydrogel with water molecules, the sodium ions were hydrated, reducing their attraction toward the carboxylate ions of PAA chains. This made the sodium ions mobile throughout the network, thereby causing the generation of osmotic pressure within the gel. However, the mobile sodium ions are weakly attracted toward the negative carboxylate ions in the polymeric backbone and the polymeric chains act as a semipermeable membrane that surrounded the sodium ions [26].

Hence, the possible driving force for swelling was coerced by the difference in osmotic pressure inside and outside the polymeric membrane. A liquid medium like water penetrated the polymeric chains of the gel, causing swelling by an expansion of their 3D

molecular networks. However, this 3D molecular network due to the presence of cross-link points prevented the chains to swell up to infinitely, thereby restricting to dissolution of the hydrogel in the medium. Moreover, the elastic contraction forces of the hydrogel network also prevent the restriction of complete solubilization of the gel, as they become more rigid than their originally coiled-shaped position. When the elastic contraction forces of the molecular network and the repulsive force of the carboxylate ions reached equilibrium, the water absorbency of SAH becomes maximum [27, 28].

2.3.4.4. Effect of salt

The swelling value of the hydrogel decreases drastically with the increase in salt concentration in the liquid medium. The swelling capacities of SAH with monovalent salt like NaCl (0.01, 0.03, and 0.09%) and with bivalent salt like $CaCl_2$ (0.01%) were found to be 61.94, 42.71, 27.00, and 2.67 g/g, respectively. Due to the difference in chemical potential and vapor pressure between the two phases, the liquid starts to move from the pure state to the solution phase. The driving force for the swelling process is the presence of osmotically active mobile counter ions. The highest degree of swelling was observed when the free Na^+ ions remain inside the hydrogel to neutralize the charges on the network of the polymeric chains. When the hydrogel was allowed to swell in a salt solution, higher numbers of ions (Na^+ or Ca^{2+}) surround the hydrogel. Consequently, the numbers of ions inside the gel are lower than the outside. As a result, the driving force for swelling of the molecular chains decreases with the increase in the salt solution. In such cases, the water from inside the hydrogel comes out, and hence, the swelling value decreased. This leads to the shrinkage of the network structure of the hydrogel and deswelling occurs to a great extent [29]. Moreover, in the case of $CaCl_2$, the bivalent cation (Ca^{2+}) has two times higher charge than Na^+; also, it has a much lower size than Na^+ ion. The combined effect of size and charge can extremely increase the number of ions outside the hydrogel than NaCl in their same concentrations, and as a result, a drastic lowering of swelling was observed in the case of $CaCl_2$.

2.3.5. Biodegradation by soil burial method

The retention of non-biodegradable hydrogel for a long time after service causes both soil and environmental pollution [30]. Thus, to utilize a material for agricultural applications, the material must be biodegradable. Our starch-based SAH due to its large amount of bio-based component leads to significant biodegradation (weight loss of 40%

within 3 months of exposure) compared with the synthetic superabsorbent, PAA hydrogel. Biodegradation under soil burial can be attributed due the microbial attack of the microorganisms that are present in the soil. It is obvious that the first step is due to the degradation of the bio-based component [1]. But there may have the possibility of hindrances caused by the synthetic poly(acrylic acid) moiety. This fact is well supported by the weight loss of different compositions of hydrogels shown in **Figure 2.6.a.** It is seen from the figure that, the weight loss decreased with an increase in the amount of AA. Moreover, the SEM images of SAH 2 before and after degradation (within 3 months) are shown in **Figure 2.6.(b-c).** It is seen that the surface morphology of the hydrogel was completely changed after degradation. Surface erosion is clearly visible in the degraded SAH 2 sample which confirmed the biodegradation of the hydrogel.

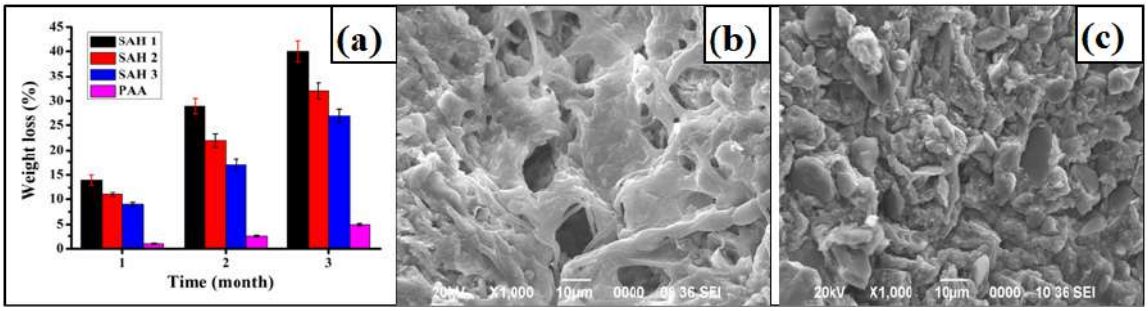

Figure 2.6. (a) Weight loss of hydrogels after 3 months, (b) SEM images of the hydrogel before degradation, and (c) SEM images of the hydrogel after degradation.

2.3.6. Determination of water-holding capacity of soil

After treatment with hydrogel, water-holding capacity of the tested soil markedly increased. The water-holding capacity of the soil was found to be significantly increased upon the incorporation of a minute dose of the hydrogel (**Figure 2.7.a**). The water-holding capacity of the untreated soil was 44%, while upon addition of only 0.1% of the hydrogel, the holding capacity was improved by 53.94%, 71.00%, and 58.34% for SAH 1, SAH 2, and SAH 3, respectively. However, SAH 2 has the highest water-absorbing capacity; hence it can enhance the water-holding capacity of the selected soil more than the others. Thus, this fact supports that hydrogel can exhibit its swelling ability in the soil also and hence can be applied for agricultural applications.

2.3.7. Determination of the density and the porosity of the soil

The particle density of the soil, which is a fixed characteristic of any kind of soil, was

found to be 2.63 g/cm^3. However, a noticeable difference was observed in the bulk density of the treated soil compared with the control. The bulk density of the hydrogel-treated soil decreased to 10.34%, 12.42%, and 11.30% for SAH 1, SAH 2, and SAH 3, respectively (**Figure 2.7.b**), compared with the bulk density of the untreated soil (1.28 g/cm^3). Based on these values of particle density and bulk density of the control and the treated soils, the porosity of the soil was obtained as shown in (**Figure 2.7.c**).

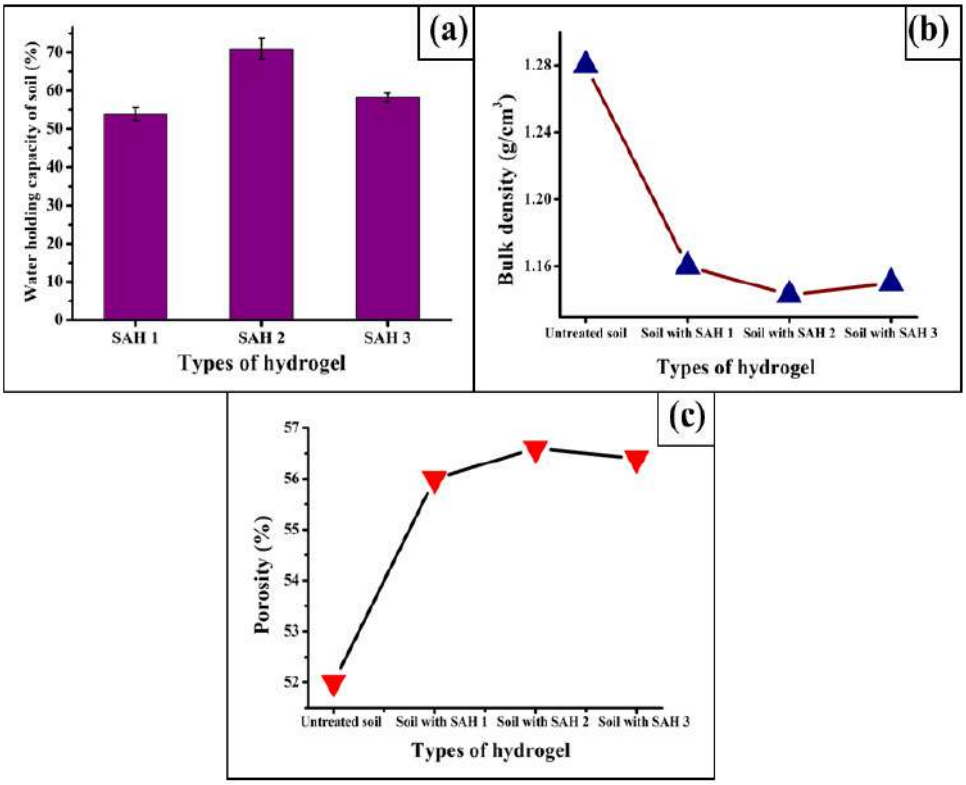

Figure 2.7. Effect of hydrogel on soil properties (a) water absorption capacity of the soil, (b) bulk density, and (c) porosity.

The selected soil for this experiment has a porosity of 52%, whereas the porosity of the hydrogel-treated soil becomes 56%, 56.6%, and 56.4% for SAH 1, SAH 2, and SAH 3, respectively. Lowering the particle density increased the porosity, as volume increased for the same weight. An increase in the porosity of the soil is more beneficial to plant growth, as with the increase in the pore size, more oxygen and nutrients can be hold for the growth of the plant. The incorporation of swollen hydrogels into the soil increases spaces among the soil particles and this leads to an increase in porosity. More swelling leads to more space, resulting in an enhancement in porosity. Hence, SAH 2-treated soil has the highest porosity. But the difference was only marginal as the amount of hydrogels incorporated in the soil samples was the same.

2.3.8. Controlled release of urea

The FTIR spectra of bare urea and urea-encapsulated hydrogel (before and after the release of urea) are given in **Figure 2.8.a**. The characteristic bands of urea at 1628 cm^{-1} and 1669 cm^{-1} for the amide carbonyl linkage and the bands at 1456 cm^{-1} for the C─N stretching frequency were observed only in the case of urea and urea-encapsulated hydrogel. But the same was absent or diminished significantly after the release of urea [16]. These results clearly indicated the successful loading and release of urea into and from the hydrogel. The hydrogel showed very high encapsulation efficiency (99.87%) and a controlled release profile in water **Figure 2.8.b**. The release performance of the hydrogel depends upon the cross-linking density of the gel. The urea holds by the hydrogel diffused through the network is due to the difference in the osmotic pressure inside and outside the gel. At the early stage, 25±2.2% of the urea was released within 5 days. During the period of 5-20 days, more than 64±4.1% of urea was released, while in 20-30 days, the release percentage was 90±2.4%. Further, with the increasing exposure time, the gel strength of the SAH decreased and the 3D network of the gel is weakened, and it may be disintegrated to some extent into smaller fragments, and hence, all the remaining urea could be also released [31].

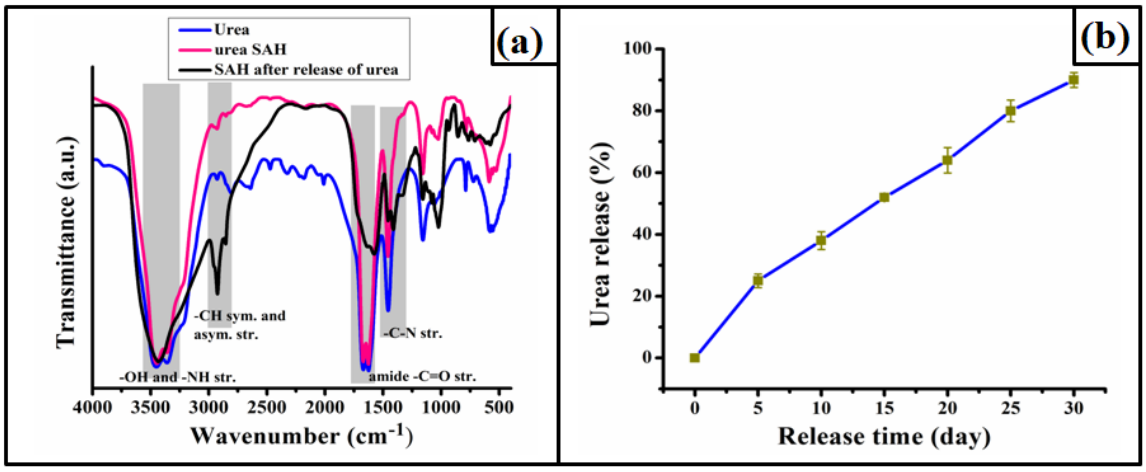

Figure 2.8. (a) FTIR spectra of urea, urea-loaded SAH, and hydrogel after release of urea, and (b) release profile of urea from encapsulated hydrogel in static water.

2.4. Conclusion

The present work described the synthesis of a biodegradable hydrogel with high water-absorbing capacity through a solution polymerization technique using water as the medium. The structure of the hydrogel was supported by spectroscopic analyses. Owing

to the optimum combination of natural polysaccharides and a synthetic polymer, the synthesized hydrogel exhibited all the requirements including biodegradability for qualifying it as a potential candidate for agricultural application. The incorporation of a very little amount of this hydrogel in the soil improved the water-holding capacity significantly. After the addition of the hydrogel, the porosity of the soil also increased significantly, this facilitates the growth of the plant. The preparation of urea-encapsulated hydrogel was also another significant outcome of this work. Further, it has extraordinary encapsulation efficiency of urea, and also the controlled release of urea can be achieved. Therefore, this research paves a direction for obtaining biodegradable hydrogel with high water-holding and nutrient-carrier ability.

References

[1] Ni, B., Liu, M., Lü, S., Xie, L., and Wang, Y. Multifunctional slow-release organic-inorganic compound fertilizer. *Journal of Agricultural and Food Chemistry*, 58(23):12373-12378, 2010.

[2] Zohuriaan-Mehr, M. J., Omidian, H., Doroudiani, S., and Kabiri, K. Advances in non-hygienic applications of superabsorbent hydrogel materials. *Journal of Materials Science*, 45(21):5711-5735, 2010.

[3] Vashist, A., Vashist, A., Gupta, Y. K., and Ahmad, S. Recent advances in hydrogel based drug delivery systems for the human body. *Journal of Materials Chemistry B*, 2(2):147-166, 2014.

[4] Tan, R., She, Z., Wang, M., Fang, Z., Liu, Y., and Feng, Q. Thermo-sensitive alginate-based injectable hydrogel for tissue engineering. *Carbohydrate Polymers*, 87(2):1515-1521, 2012.

[5] Fan, J., Shi, Z., Lian, M., Li, H., and Yin, J. Mechanically strong graphene oxide/sodium alginate/polyacrylamide nanocomposite hydrogel with improved dye adsorption capacity. *Journal of Materials Chemistry A*, 1(25):7433-7443, 2013.

[6] Demirbilek, C., and Dinç, C. Ö. Synthesis of diethylaminoethyl dextran hydrogel and its heavy metal ion adsorption characteristics. *Carbohydrate Polymers*, 90(2):1159-1167, 2012.

[7] Li, L., Wang, Y., Pan, L., Shi, Y., Cheng, W., Shi, Y., and Yu, G. A. nanostructured conductive hydrogels-based biosensor platform for human metabolite detection. *Nano Letters*, 15(2):1146-1151, 2015.

[8] Fonn, D., MacDonald, K. E., Richter, D., and Pritchard, N. The ocular response to extended wear of a high Dk silicone hydrogel contact lens. *Clinical and Experimental Optometry*, 85(3):176-182, 2002.

[9] Thombare, N., Mishra, S., Siddiqui, M. Z., Jha, U., Singh, D., and Mahajan, G. R. Design and development of guar gum based novel, superabsorbent and moisture retaining hydrogels for agricultural applications. *Carbohydrate Polymers*, 185:169-178, 2018.

[10] Cavalieri, F., Chiessi, E., Finelli, I., Natali, F., Paradossi, G., and Telling, M. F. Water, solute, and segmental dynamics in polysaccharide hydrogels. *Macromolecular Bioscience*, 6(8):579-589, 2006.

[11] Prabaharan, M., and Mano, J. F. Stimuli-responsive hydrogels based on polysaccharides incorporated with thermo-responsive polymers as novel biomaterials. *Macromolecular Bioscience*, 6(12):991-1008, 2006.

[12] Chandrika, K. P., Singh, A., Sarkar, D. J., Rathore, A., and Kumar, A. pH-sensitive crosslinked guar gum-based superabsorbent hydrogels: Swelling response in simulated environments and water retention behavior in plant growth media. *Journal of Applied Polymer Science*, 131(22):41060, 2014.

[13] Thombare, N., Mishra, S., Siddiqui, M. Z., Jha, U., Singh, D., and Mahajan, G. R. Design and development of guar gum based novel, superabsorbent and moisture retaining hydrogels for agricultural applications. *Carbohydrate Polymers*, 185:169-178, 2018.

[14] Erizal, E. Synthesis of poly (acrylamide-co-acrylic acid)-starch based superabsorbent hydrogels by gamma radiation: study its swelling behavior. *Indonesian Journal of Chemistry*, 12(2):113-118, 2012.

[15] Zhan, X. Y., Wang, F., Li, X. W., and Wang, M. Synthesis of montmorillonite/acrylic acid/acrylamide tricopolymer and its super absorbent properties. *Polymers and Polymer Composites*, 22(5):489-494, 2014.

[16] Hedrick, R. M. and Mowry, D. T. Effect of synthetic polyelectrolytes on aggregation, aeration, and water relationships of soil. *Soil Science*, 73(6):427-442, 1952.

[17] Shaviv, A. and Mikkelsen, R. L. Controlled-release fertilizers to increase efficiency of nutrient use and minimize environmental degradation-A review. *Fertilizer Research*, 35:1-12, 1993.

[18] Dutta, S., Karak, N., Saikia, J. P., and Konwar, B. K. Biodegradation of epoxy and MF modified polyurethane films derived from a sustainable resource. *Journal of Polymers and the Environment*, 18:167-176, 2010.

[19] Dutta, G. K. and Karak, N. One-pot synthesis of bio-based waterborne polyester as UV-resistant biodegradable sustainable material with controlled release attributes. *ACS Omega*, 3(12):16812-16822, 2018.

[20] Zhang, M., Song, L., Jiang, H., Li, S., Shao, Y., Yang, J., and Li, J. Biomass based hydrogel as an adsorbent for the fast removal of heavy metal ions from aqueous solutions. *Journal of Materials Chemistry A*, 5(7):3434-3446, 2017.

[21] Tomar, R. S., Gupta, I., Singhal, R., and Nagpal, A. K. Synthesis of poly (acrylamide-co-acrylic acid) based superabsorbent hydrogels: study of network parameters and swelling behaviour. *Polymer-Plastics Technology and Engineering*, 46(5):481-488, 2007.

[22] Chandrika, K. P., Singh, A., Rathore, A., and Kumar, A. Novel cross linked guar gum-g-poly (acrylate) porous superabsorbent hydrogels: Characterization and swelling behaviour in different environments. *Carbohydrate Polymers*, 149:175-185, 2016.

[23] Liang, R., Yuan, H., Xi, G., and Zhou, Q. Synthesis of wheat straw-g-poly (acrylic acid) superabsorbent composites and release of urea from it. *Carbohydrate Polymers*, 77(2):181-187, 2009.

[24] Murali Mohan, Y., Sudhakar, K., Keshava Murthy, P. S., and Mohan Raju, K. Swelling properties of chemically crosslinked poly (acrylamide-co-maleic acid) hydrogels. *International Journal of Polymeric Materials*, 55(7):513-536, 2006.

[25] Singhal, R., Tomar, R. S., and Nagpal, A. K. Effect of cross-linker and initiator concentration on the swelling behaviour and network parameters of superabsorbent hydrogels based on acrylamide and acrylic acid. *International Journal of Plastics Technology*, 13(1):22-37, 2009.

[26] Li, H., Ng, T. Y., Yew, Y. K., and Lam, K. Y. Modeling and simulation of the swelling behavior of pH stimulus responsive hydrogels. *Biomacromolecules*, 6(1):109-120, 2005.

[27] Flory, P. J. Statistical mechanics of swelling of network structures. *The Journal of Chemical Physics*, 18(1):108-111, 1950.

[28] Wang, X., Zhang, Y., Hao, C., Dai, X., Zhu, F., and Ge, C. Ultrasonic synthesis and properties of a sodium lignosulfonate–grafted poly (acrylic acid-co-acryl

amide) composite super absorbent polymer. *New Journal of Chemistry*, 38(12):6057-6063, 2014.

[29] Horkay, F., Tasaki, I., and Basser, P. J. Osmotic swelling of polyacrylate hydrogels in physiological salt solutions. *Biomacromolecules*, 1(1):84-90, 2000.

[30] Stahl, J. D., Cameron, M. D., Haselbach, J., and Aust, S. D. Biodegradation of superabsorbent polymers in soil. *Environmental Science and Pollution Research*, 7(2):83-88, 2000.

[31] Xiao, X., Yu, L., Xie, F., Bao, X., Liu, H., Ji, Z., and Chen, L. One-step method to prepare starch-based superabsorbent polymer for slow release of fertilizer. *Chemical Engineering Journal*, 309:607-616, 2017.